



**HAL**  
open science

## **THERMIC: a hardened temperature controller for regenerating CMOS circuits exposed to ionizing radiation**

Jean-Marc Armani, Alejandro Ureña-Acuña, Philippe Dollfus, Mariem Slimani

### ► To cite this version:

Jean-Marc Armani, Alejandro Ureña-Acuña, Philippe Dollfus, Mariem Slimani. THERMIC: a hardened temperature controller for regenerating CMOS circuits exposed to ionizing radiation. Radecs 2018 - 18th European Conference on Radiation and Its Effects on Components and Systems, Sep 2018, Göteborg, Sweden. 10.1109/RADECS45761.2018.9328696 . cea-03922951

**HAL Id: cea-03922951**

**<https://hal-cea.archives-ouvertes.fr/cea-03922951>**

Submitted on 5 Jan 2023

**HAL** is a multi-disciplinary open access archive for the deposit and dissemination of scientific research documents, whether they are published or not. The documents may come from teaching and research institutions in France or abroad, or from public or private research centers.

L'archive ouverte pluridisciplinaire **HAL**, est destinée au dépôt et à la diffusion de documents scientifiques de niveau recherche, publiés ou non, émanant des établissements d'enseignement et de recherche français ou étrangers, des laboratoires publics ou privés.

# THERMIC: a Hardened Temperature Controller for Regenerating CMOS Circuits Exposed to Ionizing Radiation

J. M. Armani, A. Urena Acuna, P. Dollfus, and M. Slimani

**Abstract**—A Radiation hardened temperature controller intended to regenerate CMOS circuits has been designed using commercial off-the-shelf components. Tested with  $^{60}\text{Co}$  gamma rays, it has shown a radiation hardness greater than 65 kGy. The hardening methodology used to design the temperature controller is validated through these results.

**Index Terms**—Temperature controller, CMOS component, regeneration, annealing, high temperature, ionizing dose.

## I. INTRODUCTION

**E**LECTRONIC systems operating in harsh radiative environments, like those found in the nuclear industry, may be severely affected by total ionizing dose (TID) exposure. In CMOS components, the cumulative ionizing dose induces interface traps creation and charge buildup in the gate and shallow trench isolation (STI) oxides that can strongly degrade the electrical characteristics of the circuit and result in a functional failure.

Several solutions have been proposed to enhance the robustness of electronic systems exposed to ionizing radiation. The main one consists in designing application specific integrated circuits (ASIC) using radiation hardened (rad-hard) microelectronic technologies [1] or commercial CMOS technologies with enclosed layout transistors (ELT) and guard rings [2], [3]. On the other side, commercial off-the-shelf (COTS) components have been successfully used when neither the development of an ASIC was needed nor the performance of available rad-hard parts was sufficient. Nevertheless COTS should pass through a radiation hardness assurance (RHA) methodology in order to guarantee their behavior under ionizing radiation.

However in extreme conditions, even such solutions for hardening the electronic systems may prove inadequate with regards to the duration of the mission. New techniques are thus required to ensure the overall system reliability. Some studies have demonstrated the efficiency of an annealing approach to extend the devices lifetime [4], [5]. For instance, in [5], the authors show that with a reasonable number of anneal cycles and a proper choice of the anneal parameters, the electrical characteristics of a CMOS image sensor (CIS) can

be regenerated, with a lifetime increased by at least a factor of 4.

In most of previous works, annealing was performed after irradiation by means of an oven or an external temperature controller. In the case of an embedded system exposed to radiation, the temperature controller itself should be hardened in order to ensure a reliable regeneration process. Usually, temperature controllers are either designed to have a high accuracy through the use of complex electronic circuits, or designed in a basic way with few components to ensure robustness at the expense of accuracy. Complex solutions may have integration issues in embedded devices, and simple ones may not guarantee the accuracy required for some specific applications. In addition hardly any device can withstand radiation exposure.

In this work we have designed and implemented THERMIC, a hardened embedded temperature controller for regenerating electronic devices during their exposure to high ionizing dose. This controller has several advantages compared to previous solutions proposed in [6], [7]: low self-heating resulting in a reduced volume (no heat sink needed), designed to operate in nuclear environments. Although the system described in [7] aims to measure TID temperature coefficients, its temperature controller is not designed to be exposed to radiation. Actually, both solutions presented in [6], [7] would undergo large degradation and possibly fatal failure when exposed to high level of ionizing dose. The present work represent a technical breakthrough for temperature controllers operating in highly radioactive environments.

This paper is organized as follows: Section II makes a brief review of CMOS components regeneration and explains the basic mechanisms involved. The design of the temperature controller is described in Section III. Section IV presents the characterization of the thermal controller and Section V discusses irradiation test results.

## II. REGENERATION OF CMOS COMPONENTS

Oxide trapped charges may remain trapped for a long time after irradiation (hours to many years), depending on conditions such as temperature and applied electric field [8]. Neutralization of trapped charge mechanisms such as tunneling and thermal emission have been largely studied [9], [10]. It was found that detrapping by tunneling is predominant at room temperature, which means a continuous but very long detrapping in steady state, while thermal emission becomes more effective for temperatures above 100 °C [8].

Manuscript received April 20, 2018.

J. M. Armani, A. Urena Acuna and M. Slimani are with the CEA, LIST, Laboratoire de Fiabilité et Intégration des Capteurs, 91191 Gif-sur-Yvette Cedex, France (e-mail: jean-marc.armani@cea.fr).

P. Dollfus is with the Centre for Nanoscience and Nanotechnology, CNRS, Univ. Paris-Sud, Université Paris-Saclay, Orsay, France (e-mail: philippe.dollfus@u-psud.fr)

The modeling of thermal neutralization is based on the assumption that charge detrapping follows a first order kinetics, where the probability  $\sigma$  of trap emission is given by [11]:

$$\sigma = Ae^{-\frac{E_a}{kT}} \quad (1)$$

where  $A$  is the frequency factor ( $s^{-1}$ ),  $E_a$  is the activation energy (eV),  $k$  is the Boltzmann constant and  $T$  is the absolute temperature (K). With this model one can estimate the time needed to detrapp charges up to a certain energy level with a fixed heating temperature. Isothermal anneal involves a time constant  $\tau = 1/\sigma$  with which it is possible to express the activation energy as a function of the frequency factor and the time constant  $\tau$ . So, replacing  $\tau$  in eq. (1), the activation energy can be expressed as [12]:

$$E_a(eV) = \frac{kT}{q} \ln(A\tau) \quad (2)$$

Figure 1 shows the plot of  $E_a$  estimated with eq. (2) as a function of the heating time for a temperature of 27 °C, 100 °C and 190 °C, respectively. Logically, annealing an irradiated device at a low temperature for a long period of time has the same effect as heating the device at a higher temperature for a shorter period of time. To illustrate this, let us choose an energy level of 0.947 eV that corresponds to an anneal of 168 hours at 100 °C as specified in the MIL-STD-883K standard, method 1019.9. This energy level can be reached with an annealing of 9,000 days at 27 °C, 168 hours at 100 °C and approximately 33 minutes at 190 °C.

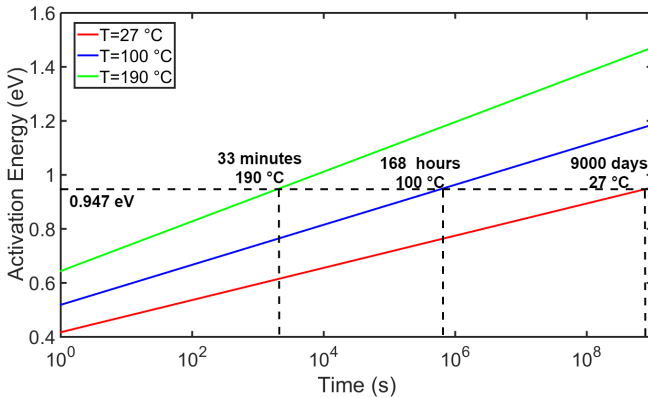


Figure 1. Time-temperature equivalence to reach a given activation energy with isothermal anneal.

The relationship between  $\sigma$  and  $E_a$  is more complex than eq. (1), but can be determined experimentally. For our calculations  $E_a$  and  $A$  were chosen from values found in the literature [12]. However, these parameters depend also on technological factors such as the foundry process. For a given component, calibration measurements may be therefore necessary to correct these values.

The control temperature accuracy can strongly influence the value of  $E_a$  achievable with an isothermal anneal. This is evidenced by differentiating eq. (1):

$$\frac{\Delta\sigma}{\sigma} = \frac{E_a}{kT} \frac{\Delta T}{T} \quad (3)$$

As the ratio  $E_a/kT$  is often high,  $\sigma$  may undergo large variations. For example, at 100 °C  $E_a/kT$  is equal to 116 for  $E_a = 1$  eV. Then, the control temperature accuracy should be very high in order to keep  $\sigma$  variation reasonably low.

Another factor that must be taken into account is the aging induced by the elevated temperature applied to the component. Aging mechanisms such as negative-bias temperature instability (NBTI), hot carrier injection (HCI), time-dependent dielectric breakdown (TDDB) and electromigration (EM) are very sensitive to temperature variation and isothermal annealing can have a significant effect on them. Moreover, thermal cycling can significantly affect the reliability of the component and lead to failure mechanisms due to thermo-mechanical fatigue stress induced by cyclic temperature fluctuations. This is particularly the case of COTS whose packages have not been designed to withstand very high temperatures. The main cause of these mechanisms is the mismatch in the coefficient of thermal expansion (CTE) of the used materials creating thermomechanical driving forces that can lead to aging of connections.

In order to minimize the impact of these phenomenon, the anneal temperature and duration, as well as the heating periodicity, should be carefully chosen. The best compromise depends especially on the final application of the system. For instance, if the system tolerates a long period of inactivity, annealing at medium temperature can be used (for example several hours at 100 °C). On the other hand, if the system only undergoes very short shutdown times, rapid annealing at high temperature must be applied. Obviously, the more frequent the annealing cycles, the faster the system will age. Nevertheless, the useful lifetime of the system under radiation could be significantly extended.

### III. DESIGN OF THE TEMPERATURE CONTROLLER

#### A. Specifications

As seen in Section II, a precise control of heating is essential when regenerating an irradiated component. On one hand, it is necessary to set accurately the temperature in order to detrapp all charges in the oxides from traps located below the suitable activation energy level. This level can be predetermined using isochronal annealing experiments. On the other hand, the temperature should remain stable during heating cycles despite the possible radiation effects on the electronic circuits of the controller. This ensures that the heated component will not be damaged by an uncontrolled rise of temperature.

The technical requirements for the temperature controller have been specified taking into account these remarks. The controller has to be compatible with a standard resistance temperature detector (RTD) while covering a temperature range of 150 °C with a heating resistor value of a few ohms. The controller should be hardened up to a cumulated dose of 50 kGy and should work properly with a 15 W DC power supply. In addition, the controller should use the pulse width modulation (PWM) principle for generating power into the heating resistor. This avoids the use of a heat-sink and therefore reduces the overall dimensions.

The temperature sensor and the heating resistor are external elements that must be thermally coupled altogether with the

component to be regenerated. To achieve this coupling, a thermal compound can be used.

### B. Design and architecture

In order to define the output power range of the temperature controller proposed in this work, we measured several printed circuit boards (PCBs) with different sizes to characterize their thermal response. On those PCBs the heating resistor was made with two surface mount device (SMD) resistors of a few ohms in series.

Table I  
THERMAL MEASUREMENT ON PCBs

Parameter	PCB 1		PCB 2	
Temperature	$T_{Low}$	$T_{High}^*$	$T_{Low}$	$T_{High}^*$
Power	4.3 W	12.4 W	2.7 W	8.1 W

$$*T_{High} = T_{Low} + 150\text{ }^{\circ}\text{C}$$

With the temperature values measured on the PCBs, we evaluated the power needed for heating at the low and high limits of the 150 °C desired temperature range. Results are shown in Table I.

After analyzing the obtained values, an output range between 2 W and 15 W was chosen to ensure a correct heating with a broad range of PCBs.

The temperature controller was designed using exclusively COTS bipolar junction transistors (BJT) in order to be able to finely adjust their configuration for achieving a high level of radiation hardness. We rejected COTS MOS transistors owing to their thick gate oxide which could trap a substantial charge and lead to an early failure of the device. Based on previous irradiation tests, BJT references were chosen among ones giving the best results in terms of radiation hardness.

The design uses extensively differential structures, which provide accurate temperature regulation together with less sensitivity to radiation induced BJT degradation. All the bias currents were fixed at a value such as the decrease of BJT weak injection gain with cumulated dose was minimal. SPICE simulations taking into account TID effects have validated these choices.

The block diagram of THERMIC controller is given in Figure 6. The temperature controller includes a voltage regulator (1), a current generator (2), a differential amplifier (3), a pulse width modulated (PWM) oscillator (4), a current switch (5), a temperature setting bridge (6), a thermal safety circuit (7), a RTD temperature sensor (10) and a heating resistor (20).

The external DC source ( $V_{cc}$ ) is transformed into a regulated output ( $V_{reg}$ ) by a linear voltage regulator made with discrete components. This regulated voltage is used by almost all functions except the current switch which is directly powered by the external DC source. The heating temperature value is set via a bridge formed by two resistors and a potentiometer, the output of which is connected to an input of the differential amplifier.

A precise current generator is used for measuring the RTD. This generator is built around a complete Wilson current mirror whose transistors are paired and integrated 2 by 2 in two packages. This ensures homogeneity of the cumulated dose

effect on the two transistors of each pair. This current mirror is thermally compensated and therefore the measurement current is at first-order independent of the temperature. In order to prevent self-heating of the RTD, the measurement current was set at a value such that the power dissipated therein remains sufficiently low.

The accuracy of the temperature controller is increased by the control loop gain provided by the differential amplifier. This one amplifies the difference between the setting voltage ( $V_{set}$ ) and the voltage across the RTD ( $V_{temp}$ ). It is built around two differential pairs whose bias currents are set by current mirrors. Results of SPICE simulations have shown an accuracy of 0.1 % with fresh components and 0.4 % with irradiated ones.

The PWM oscillator generates a square wave signal, the duty cycle of which is proportional to the output value of the differential amplifier. This signal controls the power sent into the heating resistor with the switch that chops the current drawn from the external source  $V_{cc}$ . The PWM oscillator is a relaxation oscillator whose capacitance charge current is controlled in such a way that when the input voltage increases, the duty cycle of the output signal decreases.

## IV. PROTOTYPE CHARACTERIZATION

Two prototypes of the THERMIC regulator were manufactured for testing. Figure 2 shows the PCB which has the shape of a 54 mm diameter disk. When possible, components were chosen in an SMD package for minimizing the overall size of the controller.

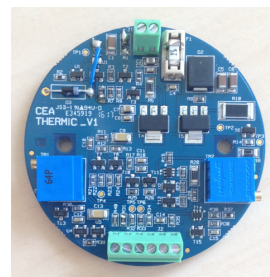


Figure 2. A prototype of the THERMIC temperature controller.

Electrical measurements have been performed on the prototypes in order to assess the performance of THERMIC controller. Results are presented in the following subsections.

### A. Accuracy

The regulation accuracy of the controller was evaluated in the upper two-thirds of the temperature set range, i.e. between ( $T_{Low} + 50\text{ }^{\circ}\text{C}$ ) and  $T_{High}$ , which corresponds to the range of temperature that will be more likely used to regenerate electronic components. The regulation error is plotted on Figure 3 as function of the set temperature. We can see that the regulated temperature slightly decreases as the controller set point is raised. Nonetheless, with a nominal power supply voltage, the error remains under 0.3 °C over the considered temperature range.

The sensitivity of the controller to power supply voltage variations around its nominal value was tested. Based on the curves ( $V_{cc} - 20\%$ ) and ( $V_{cc} + 20\%$ ), we found a value of  $0.08\text{ }^{\circ}\text{C}/\text{V}$ .

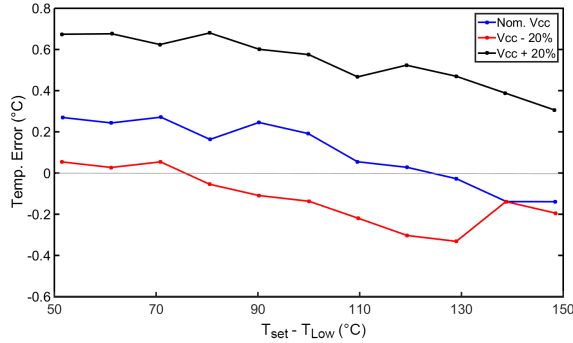


Figure 3. Regulation error for a setting in the range  $[T_{Low}+50, T_{High}]$  with different power supply voltages.

### B. Thermal sensitivity

The thermal sensitivity of the controller has been measured under stabilized temperature environment. For the experiment, one prototype previously set at a fixed point in laboratory was placed in an oven and connected to measuring instruments. We evaluated the controller's regulation error by comparing the regulated temperature to the set point. This error can be defined as:

$$E_{Reg} = T_{Reg} - T_{Set} \quad (4)$$

The oven temperature was adjusted in a range from 25 to 85  $^{\circ}\text{C}$ . The measurement results are shown in Table II.

Table II  
THERMAL STABILITY OF THE CONTROLLER

$T_{Oven}$ ( $^{\circ}\text{C}$ )	$E_{Reg}$ ( $^{\circ}\text{C}$ )
26.8	-0.22
40.4	-0.19
53.6	0.11
68.3	0.39
83.6	0.88

We can see that  $E_{Reg}$  increases with temperature, and particularly above 40  $^{\circ}\text{C}$ . The sensitivity to temperature variations in this zone is around 100 ppm/ $^{\circ}\text{C}$ .

## V. IRRADIATION TEST

### A. Experimental conditions

Irradiation of the prototypes took place in the PAGURE facility at the CEA Saclay (France). This is a gamma irradiator equipped with six  $^{60}\text{Co}$  sources (total activity of 740 TBq) placed in a 25  $\text{m}^2$  room.

The two prototypes were irradiated with a dose rate of 400 Gy/h up to a total dose of 65 kGy. As bipolar technology is prone to enhanced low dose rate sensitivity (ELDRS), a test of the controller with a low dose rate has been planned for the third quarter of 2018. Such test may be useful for devices used in nuclear power plants and subjected to low dose rates.

Before the experiment, one prototype was set at a value adapted to the PCB chosen for the experiment. The other one was set at a lower temperature so as to evaluate the influence of this parameter on the radiation damage. The voltage across the RTD and the output of the current generator were measured during the irradiation in order to characterize the behavior of the controller.

### B. Results

Figure 4 shows the plot of these two electrical parameters as functions of the cumulated ionizing dose for the prototype that was set at the lowest temperature.

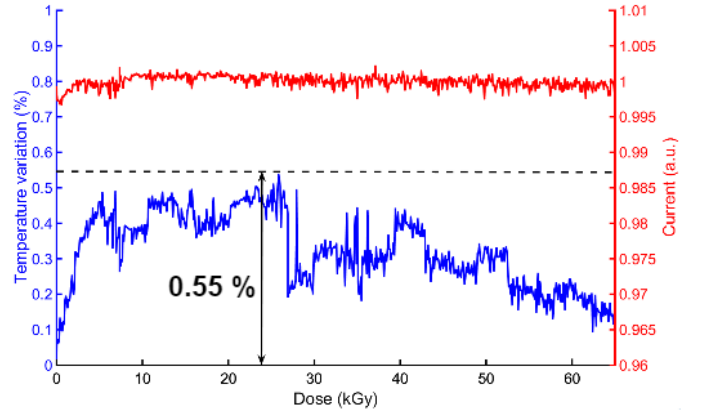


Figure 4. Evolution of the controlled temperature during irradiation for the lowest temperature setting.

The noise inherent to switched current devices is clearly visible on the curves due to the magnifying effect of the scale. We observe that the RTD current increases slightly by 0.3 % up to 10 kGy and then stabilizes. The evolution of the voltage across the temperature sensor shows a similar ascending profile during the first 10 kGy, then a stabilization until an irradiation stop at 27 kGy where the signal exhibits a negative step. After the stop, the curve increases again up to 40 kGy and finally decreases until the end. The maximum drift of temperature corresponds to a relative error of 0.55 %. This value is comparable to the 0.4 % obtained with SPICE simulations.

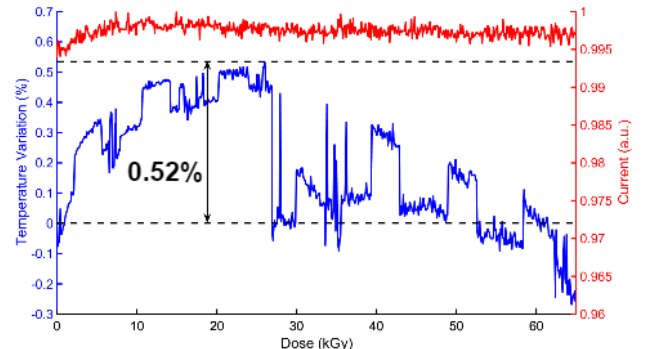


Figure 5. Evolution of the controlled temperature during irradiation for the highest temperature setting.

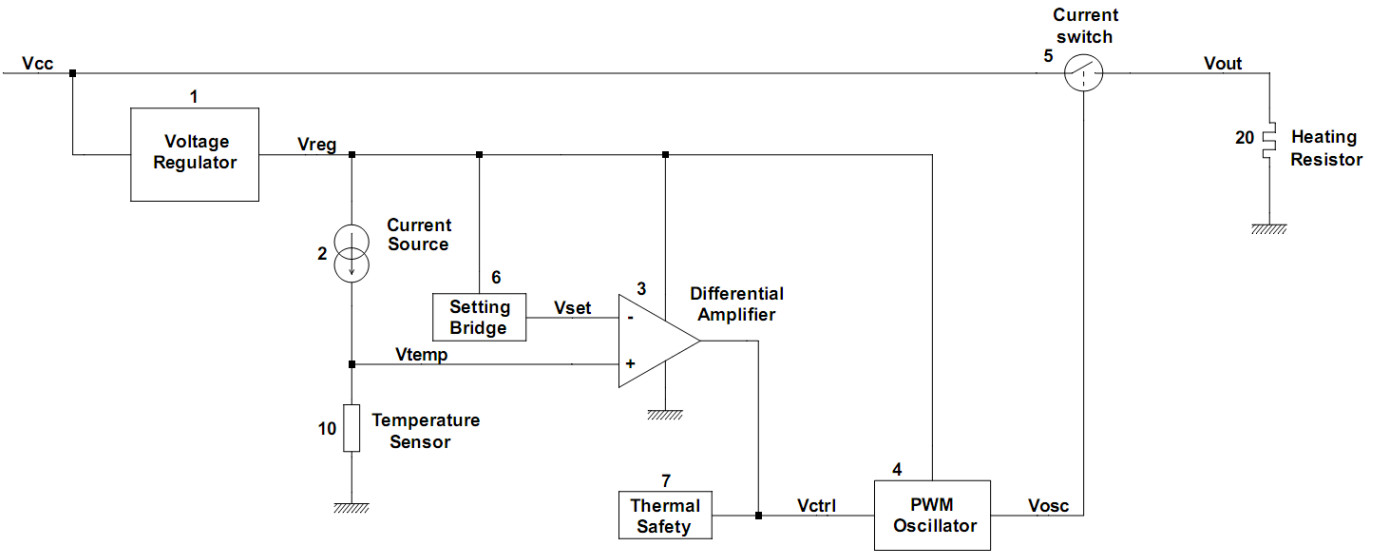


Figure 6. Block diagram of the THERMIC temperature controller.

Figure 5 shows the evolution of the two measured parameters as functions of the ionizing dose for the second prototype. We can see that the RTD current has the same variation as the first prototype and this is because the temperature setting doesn't affect the current generator. On the other hand, the voltage across the sensor has a similar shape as the first prototype but with a larger amplitude since the gain of the differential amplifier is influenced by the temperature setting. The maximum drift observed corresponds to a relative error of 0.52 %, which is again in accordance with SPICE simulation results.

## VI. CONCLUSION

The design of an embedded temperature controller built with COTS components and its experimental TID test results have been presented. Irradiation with  $^{60}\text{Co}$  demonstrates a drift of the regulated temperature lower than 0.55 % after a total dose of 65 kGy. This value is in full agreement with the SPICE simulations and totally compatible with the requirements of a hardened regeneration controller.

The total dose hardness of the temperature controller has shown to be greater than 65 kGy. This validates the hardening methodology used to design the temperature controller.

## ACKNOWLEDGMENT

This work was funded as part of a joint laboratory between CEA and ERMES Company (Saclay, France) which commercializes the THERMIC regulator.

## REFERENCES

- [1] M. Dentan, P. Abbon, E. Delagnes, N. Fourches, D. Lachartre, F. Lugiez, B. Paul, M. Rouger, R. Truche, J. Blanc *et al.*, "Dmill, a mixed analog-digital radiation-hard bicmos technology for high energy physics electronics," *IEEE Transactions on Nuclear Science*, vol. 43, no. 3, pp. 1763–1767, 1996.
- [2] R. C. Lacoë, "Improving integrated circuit performance through the application of hardness-by-design methodology," *IEEE transactions on Nuclear Science*, vol. 55, no. 4, pp. 1903–1925, 2008.
- [3] M. L. McLain, H. J. Barnaby, I. S. Esqueda, J. Oder, and B. Vermeire, "Reliability of high performance standard two-edge and radiation hardened by design enclosed geometry transistors," in *Reliability Physics Symposium, 2009 IEEE International*. IEEE, 2009, pp. 174–179.
- [4] J. Armani, P. Barrochin, F. Joffre, R. Gaillard, F. Saigné, and J. Mainguy, "Enhancement of the total dose tolerance of a commercial cmos active pixel sensor by use of thermal annealing," in *Radiation and Its Effects on Components and Systems (RADECS), 2011 12th European Conference on*. IEEE, 2011, pp. 340–344.
- [5] S. Dhombres, A. Michez, J. Boch, F. Saigne, S. Beauvivre, D. Kraehenbuehl, J.-R. Vaillé, P. Adell, E. Lorfevre, R. Ecoffet *et al.*, "Study of a thermal annealing approach for very high total dose environments," *IEEE Transactions on Nuclear Science*, vol. 61, no. 6, pp. 2923–2929, 2014.
- [6] G. Andria, G. Cavone, C. G. C. Carducci, M. Spadavecchia, and A. Trotta, "A pwm temperature controller for thermoelectric generator characterization," in *Metrology for Aerospace (MetroAeroSpace), 2016 IEEE*. IEEE, 2016, pp. 291–296.
- [7] J. Hofman, A. Holmes-Siedle, R. Sharp, and J. Haze, "A method for in-situ, total ionising dose measurement of temperature coefficients of semiconductor device parameters," *IEEE Transactions on Nuclear Science*, vol. 62, no. 6, pp. 2525–2531, 2015.
- [8] J. R. Schwank, M. R. Shaneyfelt, D. M. Fleetwood, J. A. Felix, P. E. Dodd, P. Paillet, and V. Ferlet-Cavrois, "Radiation effects in mos oxides," *IEEE Transactions on Nuclear Science*, vol. 55, no. 4, pp. 1833–1853, 2008.
- [9] D. Fleetwood, "Revised model of thermally stimulated current in mos capacitors," *IEEE Transactions on Nuclear Science*, vol. 44, no. 6, pp. 1826–1833, 1997.
- [10] P. McWhorter, S. Miller, and W. Miller, "Modeling the anneal of radiation-induced trapped holes in a varying thermal environment," *IEEE Transactions on Nuclear Science*, vol. 37, no. 6, pp. 1682–1689, 1990.
- [11] D. M. Fleetwood, P. S. Winokur, M. R. Shaneyfelt, L. C. Riewe, O. Flament, P. Paillet, and J. L. Leray, "Effects of isochronal annealing and irradiation temperature on radiation-induced trapped charge," *IEEE Transactions on Nuclear Science*, vol. 45, no. 6, pp. 2366–2374, 1998.
- [12] F. Saigné, L. Dusseau, L. Albert, J. Fesquet, J. Gasiot, J. David, R. Ecoffet, R. Schrimpf, and K. Galloway, "Experimental determination of the frequency factor of thermal annealing processes in metal-oxide-semiconductor gate-oxide structures," *Journal of applied physics*, vol. 82, no. 8, pp. 4102–4107, 1997.